Eruptivity Criteria for Magnetic Flux Ropes in the Solar Corona

Oliver Rice

Supervised by Anthony Yeates

UK Research and Innovation

Durham University

1. The Aim and Our Models

Our work focuses on predicting eruptions of magnetic flux ropes in the solar corona. This process is one of the mechanisms behind large coronal mass ejections (CMEs) and associated space weather. The eventual goal would be to use observational data to make real-time predictions of solar activity and resultant space weather, but this is a long way off!

We propose several ratios between theoretically measurable quantities that appear to correlate well with eruptive behaviour, including a modified version of the previously proposed 'eruptivity index'.

Magnetofrictional Equations

$$\nabla \cdot \boldsymbol{B} = 0$$
$$\nabla \times \boldsymbol{E} = -\frac{\partial \boldsymbol{B}}{\partial t}$$
$$\nabla \times \boldsymbol{B} = \mu_0 \boldsymbol{j}$$
$$\boldsymbol{E} = \eta \boldsymbol{j} - \boldsymbol{v} \times \boldsymbol{B}$$
$$\boldsymbol{v} = \frac{v_0 \boldsymbol{j} \times \boldsymbol{B}}{B^2 + \delta e^{-\delta B^2}} + v_{out}(y)\mathbf{e}_y$$

In our latest study we have used three translationally-invariant models: A Cartesian Magnetofrictional Model, an Axisymmetric Polar Magnetofrictional Model[1], and a Cartesian MHD model using the LARE2D code[2].

All three models are invariant in one dimension, which is far faster than full 3D and has allowed us to model thousands of individual flux ropes and eruptions in a very large parameter study.

The behaviour of the system is determined in part by conditions on the lower boundary. The sun's differential rotation causes out-of-plane shearing of the magnetic arcade, and supergranular diffusion forces the magnetic footpoints closer together, forming a flux rope (twisted bundle of magnetic flux) as in **Figure 1**.

MHD Equations

$$\nabla \cdot \boldsymbol{B} = 0$$
$$\nabla \times \boldsymbol{E} = -\frac{\partial \boldsymbol{B}}{\partial t}$$
$$\nabla \times \boldsymbol{B} = \mu_0 \boldsymbol{j}$$
$$\boldsymbol{E} = \eta \boldsymbol{j} - \boldsymbol{v} \times \boldsymbol{B}$$
$$\frac{\partial \boldsymbol{\rho}}{\partial \boldsymbol{t}} = -\boldsymbol{\nabla} \cdot (\rho \boldsymbol{v})$$
$$\frac{D\boldsymbol{v}}{Dt} = \frac{1}{\rho}\boldsymbol{j} \times \boldsymbol{B} - \frac{1}{\rho}\boldsymbol{\nabla} \mathrm{P} + \mathbf{g}$$
$$\frac{D\epsilon}{Dt} = -\frac{P}{\rho}\boldsymbol{\nabla} \cdot \boldsymbol{v} + \frac{\eta}{\rho}\boldsymbol{j}^2$$
$$\epsilon = \frac{P}{\rho(\gamma - 1)}$$

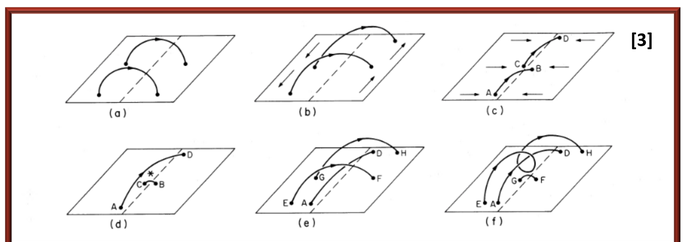

Figure 1: Formation of a magnetic flux rope, showing the effect of shearing (b) and surface diffusion (c), reconnecting at the polarity inversion line. *(From van Ballegooijen and Martens, 1989)*

2. Flux Rope Behaviour and Eruptions

We observe similar behaviour in all three models. There are two types of eruption: arcade eruptions[4], which occur in the field overlying the rope, and full flux rope eruptions - the rapid ejection of the rope itself. We focus mainly on flux rope eruptions as these are more significant.

Varying system parameters such as the initial density ρ_0 (in the MHD simulations), the magnetofrictional relaxation constant v_0 and the supergranular diffusion rate η_0 allows us to observe hundreds of flux rope eruptions of varying magnitudes.

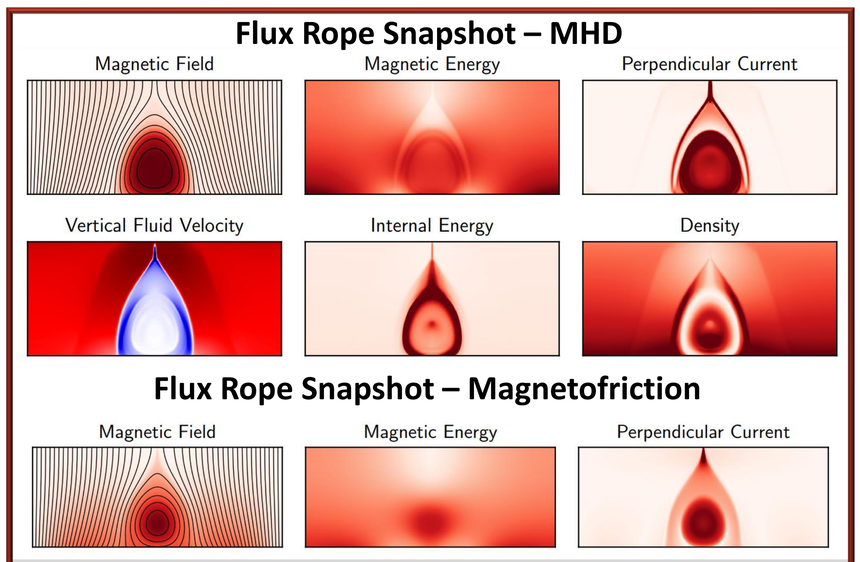

Figure 3: Snapshots of flux ropes in MHD and Magnetofriction. All values are strictly positive (red) except for the fluid velocity. In the 'Magnetic Field' pane the in-plane magnetic field is represented with black lines, and the colourmap is the out-of-plane field strength.

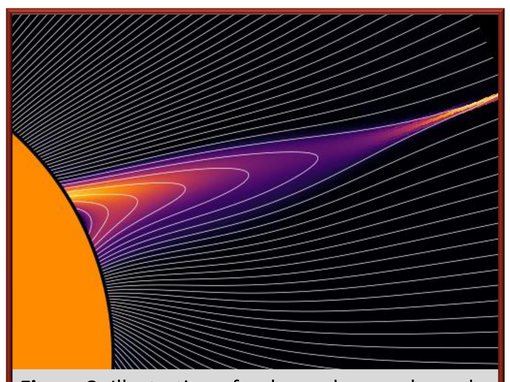

Figure 2: Illustration of a sheared coronal arcade, in one of the axisymmetric polar simulations. The heatmap here shows the out-of-plane current.

Snapshots of a flux rope in both MHD and Magnetofriction are shown in **Figure 3**. The similarity between the two models is clear, although the structure of the flux rope is more complex in full MHD.

A typical flux rope eruption is shown in **Figure 4**. The flux rope forms and is stable for some time (several hundred days, in this case). During a flux rope eruption we observe fast reconnection below the centre of the rope, and the entire structure moves quickly upwards out of the domain.

In most cases there is sufficient energy left in the system for another rope to form after an eruption, and the process repeats.

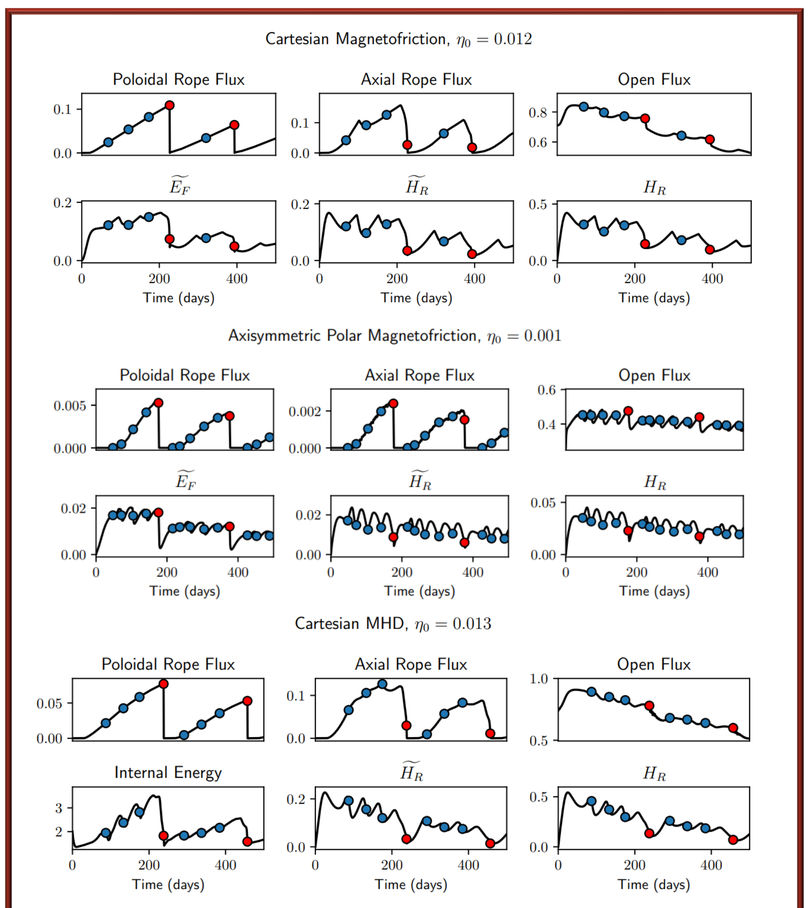

Figure 5: A selection of the scalar diagnostics we can measure. H_R is the relative helicity, which we can define in two different ways (see the panel in Section 5). η_0 is the supergranular diffusion rate – one of the variable parameters.

3. Diagnostic Measurements

A selection of the diagnostic measurements of the system is shown in **Figure 5**, for a representative simulation in each of the three models.

These diagnostics are either properties of the rope itself (eg. axial flux), or properties of the entire system, such as the total magnetic energy or open flux.

In **Figure 5** arcade eruptions are shown in blue and full flux rope eruptions in red. In general, there are repeated arcade eruptions above the rope during formation, causing most diagnostics to oscillate. After a full flux rope eruption the rope flux and current fall to zero before the rope reforms.

Some diagnostic measurements require the construction of an appropriate reference magnetic field $\boldsymbol{B}_P$. These include the free energy E_F and the relative helicity H_R, discussed in more detail in Section 5. We refer these diagnostics as 'reference-based quantities'.

Ultimately, we find that no single diagnostic measurement is itself a good predictor of flux rope eruptions, as there is never a consistent threshold at which eruptions are likely to occur.

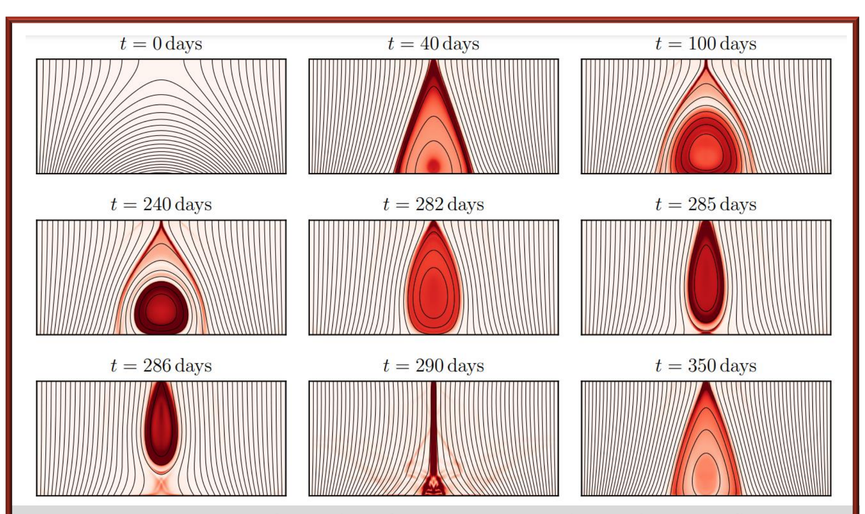

Figure 4: A sequence of snapshots from an MHD simulation showing a flux rope eruption at around t = 290 days and subsequent reformation. The colourmap represents the out-of-plane current and the black lines the in-plane magnetic field.

4. Predictive Ratios

The number of possible ratios between diagnostic measurements is enormous. Most of them make little physical sense and can be disregarded – but there are still several hundred contenders.

The best ratios tend to fall into two categories: Rope flux or current squared normalised by a reference-based quantity, or ratios between two reference-based quantities. The latter includes the `eruptivity index', discussed in more detail in Section 5.

We can evaluate the predictive ability of diagnostic ratios using histograms, as in **Figure 6.** For every snapshot across the whole parameter study (several hundred thousand!) we check whether a rope will erupt within a given time (10 days in this case) and group the ratio values to form distributions.

For instance, for the ratio on the right of the figure the peak in the red curve at around 0.6 units indicates that if this ratio has a measured value around 0.6, an eruption is very likely within 10 days. This peak is in a similar position in both MHD and magnetofriction.

We observe that certain ratios consistently reach a particular threshold at which an eruption occurs, and as such are good predictors. The accuracy of such predictions can then be quantified with a 'skill score' E. The highest skill score is for the axial current squared normalised by the relative helicity - with E = 0.968 indicating 96.8% of eruptions could theoretically be predicted using this ratio.

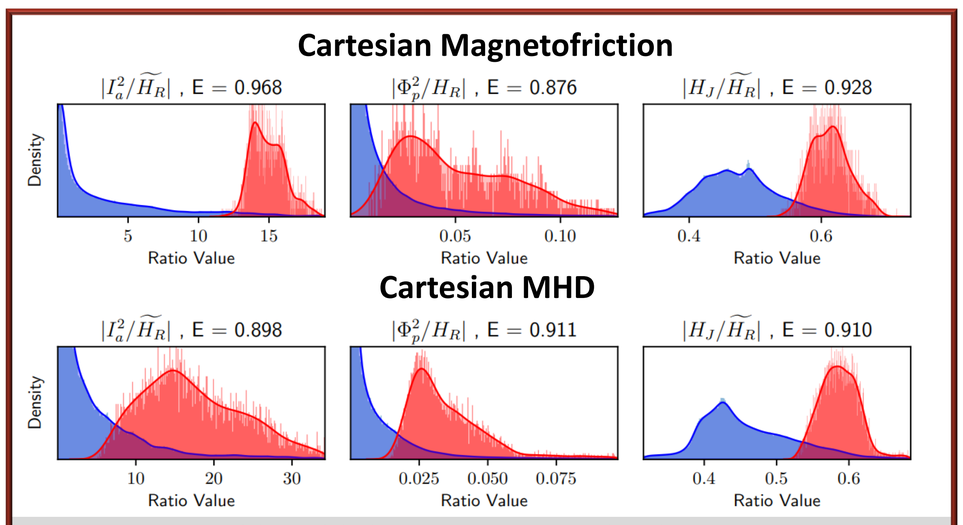

Figure 6: Histograms of three of the best predictive ratios. Values that precede eruptions within 10 days are coloured in red, and those that do not are in blue. The skill score E is an indication of how distinct the red/blue curves are, and thus the predictive ability of that ratio. Here I_a is the axial rope current, and Φ_p is the poloidal rope flux.

5. Helicity and the Eruptivity Index

One predictive ratio has consistently been proposed as a good predictor of eruptions. This is the `eruptivity index' – the ratio of current-carrying helicity to relative magnetic helicity H_J/H_R. It has been shown[5] that high values of this index tend to precede eruptive behaviour. Unfortunately, in our previous work[6] we found that this index was not at all correlated to eruptivity.

Calculating these helicities requires the construction of a reference field $\boldsymbol{B}_P$. The out-of-plane component of this field can be set either to zero, or to a constant value equal to the average out-of-plane flux (see inset).

Calculating the eruptivity index purely using either of these definitions H_J/H_R or $\tilde{H}_J/\tilde{H}_R$ does not yield positive results. But we have found that mixing the definitions - $H_J/\tilde{H}_R$ - does indeed work very well, correctly predicting up to 92% of eruptions in both magnetofriction and MHD with consistent peak values in both models (at around 0.6 units). The improvement of this new definition over the old can be seen in **Figure 7**.

Relative and Current-Carrying Helicity

$$H_R = \int (\boldsymbol{A} + \boldsymbol{A}_P) \cdot (\boldsymbol{B} - \boldsymbol{B}_P) dV$$

$$H_J = \int (\boldsymbol{A} - \boldsymbol{A}_P) \cdot (\boldsymbol{B} - \boldsymbol{B}_P) dV,$$

with $\boldsymbol{A}$ such that $\boldsymbol{B} = \nabla \times \boldsymbol{A}$.
$\boldsymbol{B}_P$ is a suitable potential field, with normal boundaries matching $\boldsymbol{B}$.

If the out-of-plane component of $\boldsymbol{B}_P$ is zero we write the respective diagnostic with no twiddle (eg. H_R). If the out-of-plane component instead equals $B_{P_z}(x,y) = \frac{1}{A}\int B_y(x,y)dxdy$, then the respective diagnostic is written with a twiddle (eg. $\widetilde{H_R}$).

6. Conclusions

We find that there are several diagnostic ratios that could be used to predict flux rope eruptions. Notable examples are the axial current squared normalised by the relative helicity, and a new variation on the previously established eruptivity index.

We also find that several conditions for flux rope eruptivity are consistent between MHD and magnetofriction, and that flux ropes behaviour is similar in both cartesian and axisymmetric polar models.

It remains to test these theories in full 3D, and to establish methods for measuring predictive ratios from observed data.

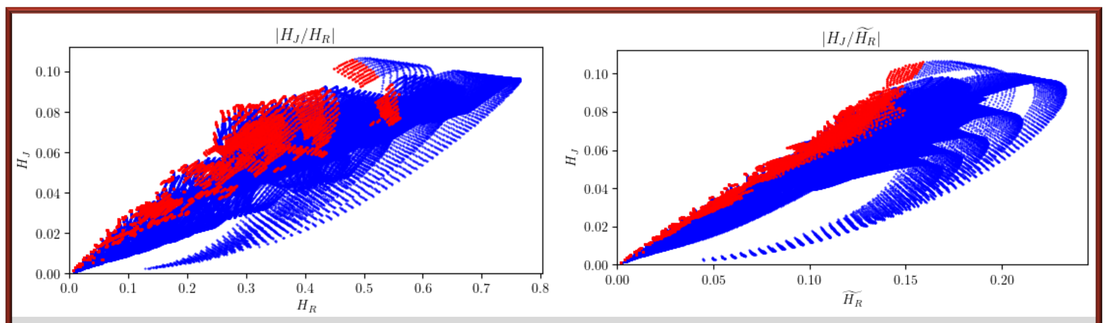

Figure 7: Scatter plots of the relative helicity and current-carrying helicity. If a rope will erupt within 10 days, the point is coloured red. The standard definition of eruptivity index is the left pane, with our modified version on the right. The linear correlation of the red points indicates a consistent ratio value at which eruptions occur.

References

[1] Mackay, D. H., & Yeates, A. R. 2012, Living Reviews in Solar Physics, 9, 6
[2] Arber et al. 2001, Journal of Computational Physics, 171, 151
[3] van Ballegooijen, A. A., & Martens, P. C. H. 1989, The Astrophysical Journal, 343, 971
[4] Bhowmik, P., & Yeates, A. R. 2021, SoPh, 296, 109
[5] Pariat, E., Leake, J. E., Valori, G., et al. 2017, Astronomy & Astrophysics, 601, A125
[6] Rice, O. E. K., & Yeates, 2022, Frontiers in Astronomy and Space Sciences, 9, 849135